C-end rule peptides mediate neuropilin-1-dependent cell, vascular, and tissue penetration

Tambet Teesalu[a,1,2], Kazuki N. Sugahara[a,1], Venkata Ramana Kotamraju[a], and Erkki Ruoslahti[a,b,2]

[a]Vascular Mapping Center, The Burnham Institute for Medical Research at University of California, Santa Barbara, CA 93106-9610; and [b]Cancer Research Center, The Burnham Institute for Medical Research, La Jolla, CA 92037

Contributed by Erkki Ruoslahti, July 24, 2009 (sent for review May 29, 2009)

Screening of phage libraries expressing random peptides for binding to prostate cancer cells primarily yielded peptides that had a C-terminal arginine (or rarely lysine) residue, usually in a consensus context R/KXXR/K. Phage expressing these sequences and synthetic nanoparticles coated with them bound to and were internalized into cells. The C-terminal arginine (or lysine) was essential to the activity; adding another amino acid, or even blocking the free carboxyl group of this arginine residue by amidation, eliminated the binding and internalizing activity. An internal R/KXXR/K can be exposed and switched on by a cleavage by a protease. The strict requirement for C-terminal exposure of the motif prompted us to term the phenomenon the *C-end rule* (CendR). Affinity chromatography showed that the CendR peptides bind to neuropilin-1 (NRP-1) on the target cells. NRP-1 is a cell-surface receptor that plays an essential role in angiogenesis, regulation of vascular permeability, and the development of the nervous system. VEGF-A165 and other ligands of NRP-1 possess a C-terminal CendR sequence that interacts with the b1 domain of NRP-1 and causes cellular internalization and vascular leakage. Our CendR peptides have similar effects, particularly when made multivalent through coupling to a particle. We also noted a unique and important activity of these peptides: penetration and transportation through tissues. The peptides were able to take payloads up to the nanoparticle size scale deep into extravascular tissue. Our observations have implications in drug delivery and penetration of tissue barriers and tumors.

homing peptides | vascular permeability | VEGF | cell penetrating peptides

Penetration of macromolecules and supramolecular complexes into cells and through tissue barriers is a recurrent theme in a multitude of physiologic and pathologic processes. The cell membrane and vascular wall barriers to entry into cells and tissues can be penetrated in a number of ways. Some cellular and microbial proteins are capable of penetrating from outside a cell into the cytoplasm. Examples of such proteins include homeodomain transcription factors such as Antennapedia (1), the herpes simplex virus-1 protein VP22 (2), and the HIV-1 transactivator Tat protein (3, 4). Short cationic cell-penetrating peptides (CPPs) derived from these proteins retain their ability to internalize into cells and can carry along cargoes such as proteins, nucleic acids, and nanoparticles (5). The CPPs are not selective; they are taken up into nearly all types of cells. Internalizing peptides that are tissue specific have also been described (6–9). CPP derivatives with cationic and anionic modules linked by a protease-sensitive linker have been developed for tumor-selective delivery (10). The mechanisms of the cellular uptake of the various CPPs are incompletely understood.

Blood vessels in an adult organism are generally impermeable to macromolecules. Certain macromolecules are actively transported across vascular walls (11). Increased vascular permeability (i.e., "leakiness") of vessels and accumulation of plasma components in the interstitium is associated with physiologic angiogenesis, for example during embryonic development (12). Vascular leakage is also a characteristic of tumor vessels, where it is the cause of the so-called enhanced permeability and retention effect (13). VEGF is, at least partly, responsible for the leakiness of angiogenic vessels (13, 14). VEGF was originally described as a tumor-secreted vascular permeability factor (15) and later independently cloned as an endothelial cell mitogen (16, 17). Neuropilin-1 (NRP-1) is a hub receptor with multiple ligands that plays an essential role in angiogenesis and cardiovascular development (18, 19). NRP-1 is required for induction of vascular permeability by VEGF (20) and semaphorin 3A (21). Both VEGF and semaphorin 3A interact with the b1 domain of NRP-1 using their C-terminal basic domains, and synthetic peptides homologous to the VEGF-A165 C terminus block the VEGF–NRP-1 interaction and its biologic effects (22, 23).

Here, we describe a class of peptides derived from phage display screens that induce cell internalization and tissue penetration. These peptides share a R/K/XXR/K motif with the C-terminal domains of VEGF-A165 and some semaphorins and bind to NRP-1. The R/KXXR/K motif must be exposed at the C terminus of a polypeptide chain for the motif to be active (hence the term *C-end rule* or CendR). We also show that a cryptic R/KXXR/K motif embedded in a protein or peptide sequence can be activated by a protease. Our findings uncover a penetration switch that is likely to be useful in targeted drug delivery and possibly also in modulating biologic processes involving vascular leakage and cell internalization for therapeutic purposes. Because tumor cells overexpress NRP-1, this approach may be particularly applicable to drug delivery into tumors.

Results

Identification and Characterization of a C-Terminal Internalization Element. We used T7 phage display (24) to identify peptides that home to PPC-1 human prostate carcinoma xenograft tumors. As an initial step, we performed 3 rounds of *ex vivo* selection and obtained selected phage pools that bound to PPC-1 cells ≈500-fold over the control phage. To our surprise, independent of the structure of the initial libraries, which included a cyclic CX7C library (C, cysteine; X, any amino acid) and a linear X7 library, the peptides in the selected phage pool almost universally contained a C-terminal arginine (or in some cases, lysine) residue (Fig. S1*A*). The terminal basic residue was often preceded by another R/K in a consensus R/KXXR/K. In a subsequent screening using a constrained library with the RXXR as a fixed element (RXXRXXX library) we found that a tandem RXXR motif, such as RPARPAR, RGERPPR, and RVTRPPR, was particularly efficient in promoting phage binding (>1,000-fold over control phage; Fig. S1). The structural similarity of the peptides and their ability to compete with each other (Fig. S2) implied a shared binding mechanism. To understand the function of the R/KXXR/K motif, we used the prototypic RPARPAR peptide for subsequent studies.

The RPARPAR phage bound to the PPC1 cells was also

Author contributions: T.T., K.N.S., V.R.K., and E.R. designed research; T.T., K.N.S., and V.R.K. performed research; V.R.K. contributed new reagents/analytic tools; T.T., K.N.S., and E.R. analyzed data; and T.T., K.N.S., and E.R. wrote the paper.

The authors declare no conflict of interest.

[1]T.T. and K.N.S. contributed equally to this work.

[2]To whom correspondence may be addressed. E-mail: tteesalu@burnham.org or ruoslahti@burnham.org.

This article contains supporting information online at www.pnas.org/cgi/content/full/0908201106/DCSupplemental.

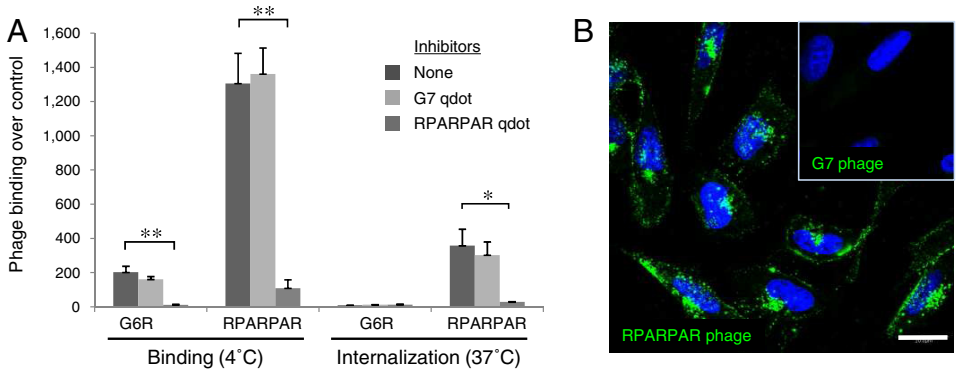

Fig. 1. Interaction of and RPARPAR phage with cultured PPC-1 cells. (*A*) Cells were incubated with phage at 4 °C to assess surface binding or at 37 °C, followed by a wash at low pH, to assess phage internalization. RPARPAR-functionalized qdots inhibited both the binding and internalization of RPARPAR phage, whereas G7 qdots had no effect. GGGGGGR (G6R) phage was only minimally internalized. The binding of G6R phage to PPC-1 cells was blocked by an excess of RPARPAR qdots. Binding is expressed as fold over control G7 phage. Statistical analysis was performed by Student's *t* test. $n = 3$; error bars indicate SEM; *, $P < 0.05$; **, $P < 0.01$. (*B*) Confocal microscopic images of PPC-1 cells incubated for 2 h at 37 °C with phage displaying RPARPAR or G7 (*Inset*) peptide. The phage was detected by staining with an anti-T7 phage polyclonal antibody. Green, phage; blue, DAPI. (Scale bars, 20 μm.)

internalized into the cells at 37 °C (Fig. 1). Quantum dots (qdots) coated with synthetic RPARPAR peptide also bound to the cells and internalized into them. Live cell imaging showed that at 37 °C the RPARPAR qdots associate with plasma membrane in 15 min and accumulate in the perinuclear area by 1 h after addition to the cells (Fig. S3*A*). Mutagenesis of RPARPAR showed that a C-terminal arginine (or lysine) is critical for the initial binding of the phage to cells and that the other 2 basic amino acids increase the interaction in a dose- and position-dependent manner, contributing to the subsequent internalization (Fig. 1*A* and and Fig. S1*B*). Capping the C-terminal R with an additional C-terminal amino acid (as in RPARPARA) abolished the binding of the phage and qdots to the cells (Figs. S1*B* and S3*B*). Even amidation of the C-terminal carboxyl group in the RPARPAR peptide eliminated the cell binding, as shown by using qdots coated with such a peptide (Fig. S3*B*). The strict requirement for C-terminal exposure of a basic amino acid for activity prompted us to term the R/KXXR/K peptides the C-end rule (CendR) peptides. We hypothesized that proteolysis could be used to activate internal CendR elements (Fig. 2*A*). To test this, we treated the RPARPARA phage with trypsin, which cleaves at basic residues. Trypsin treatment increased the binding of the RPARPARA phage to cells by 110 ± 10-fold (Fig. 2*B*). Thus, an internal CendR motif can serve as a cryptic binding site that can be activated by a proteolytic switch.

The CendR mechanism of peptide binding and uptake was present in all 4 tumor cell lines we tested, vascular endothelial cells, and in primary cells derived from normal mouse organs (Fig. S4). Intravenously injected RPARPAR phage accumulated strongly in the first-met vascular beds: in the lungs and, to a lesser extent, the heart (Fig. 3*A*). We found immunoreactivity for RPARPAR phage, but not control phage, throughout lung tissue, indicating that the RPARPAR phage penetrates into tissue parenchyma (Fig. 3*B*).

We next tested a panel of inhibitors of various endocytosis pathways for their ability to inhibit cellular uptake of RPARPAR. None of these inhibitors, which included chlorpromazine (clathrin-dependent uptake), genistein and nystatin (caveolar endocytosis), and [5-(*N*-ethyl-*N*-isopropyl)]amiloride and wortmannin (macropinocytosis), blocked the uptake of RPARPAR phage (Fig. S5*A*). Moreover, the internalized RPARPAR phage did not colocalize with any of the subcellular compartments detected with a panel of available antibody probes (Fig. S5*B*).

Many cationic CPPs, such as the TAT peptide derived from HIV-1 transactivator protein, contain internal or exposed CendR elements and C-terminal basic amino acids. The initial binding of a phage clone engineered to display the TAT peptide (RKKRRQRRR) to PPC1 cells was inhibited by the addition of free RPARPAR peptide (binding 38% ± 7% of no-competitor control) or RPARPAR qdots (binding 4% ± 2% of control), indicating that the CendR binding/internalization pathway may be at least partly responsible for the activities of the TAT peptide (Fig. S6). The CPPs are active when synthesized using D-amino acids (10, 25, 26). We tested an RPARPAR peptide comprising D-amino acids (D-rparpar) and found that qdots coated with this peptide did not bind to or internalize into cells (Fig. S3*B*). These results indicate that, unlike the CPPs, the CendR peptide uses a chiral binding site.

RPARPAR Peptide Interacts with NRP-1. To identify RPARPAR-interacting cellular proteins, we fractionated extracts of PPC-1 tumor

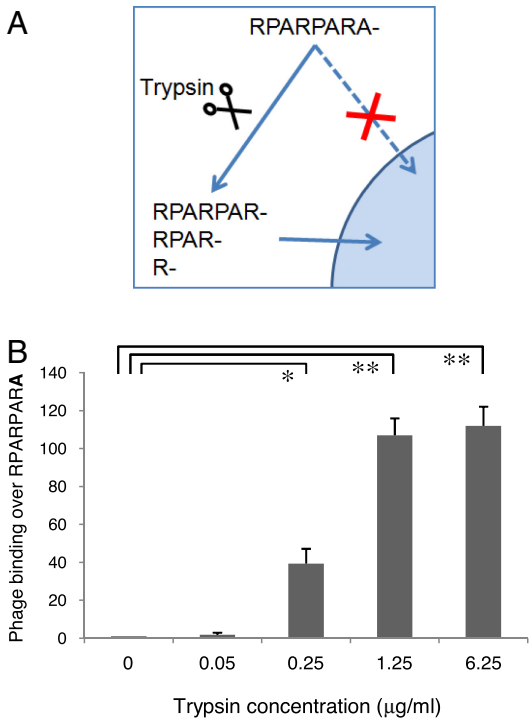

Fig. 2. Proteolytic activation of CendR peptides. (*A*) Scheme of activation of cryptic RPARPARA peptide by tryptic digestion. Trypsin cleaves after basic amino acids to expose C-terminal arginine residues. (*B*) Binding of RPARPARA-displaying phage is enhanced by trypsin treatment. Statistical analysis was performed with ANOVA; $n = 3$; error bars indicate SEM; *, $P < 0.05$; **, $P < 0.01$.

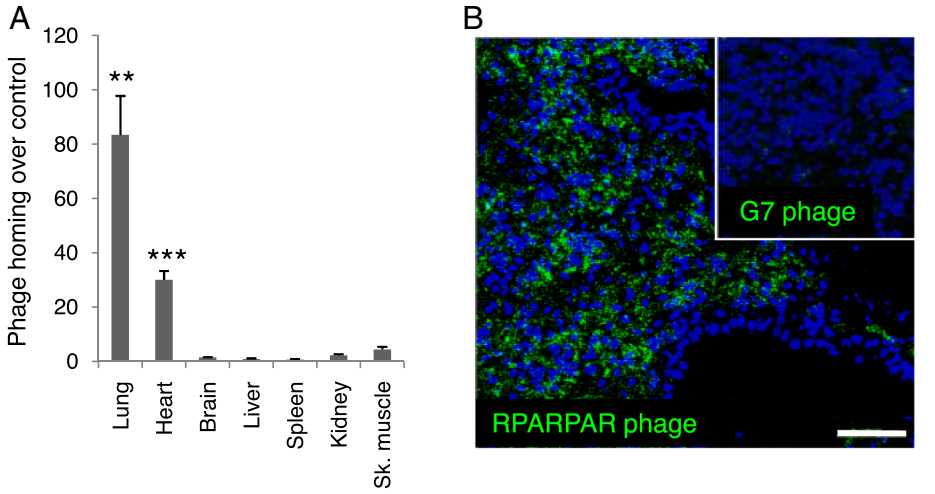

Fig. 3. (*A*) Tissue distribution of i.v. injected RPARPAR phage after 20 min of circulation. The titer of RPARPAR phage is expressed as fold over control G7 phage. Statistical analysis was performed by Student's *t* test. $n = 3$; error bars indicate SEM; **, $P < 0.01$; ***, $P < 0.001$. (*B*) Immunofluorescent localization of phage (green) in lung sections of mice injected i.v. with RPARPAR or G7 (*Inset*) phage. The RPARPAR phage shows widespread phage immunoreactivity in lung tissue, whereas no control G7 phage is detected. (Scale bar, 50 μm.)

xenograft tumors by affinity chromatography on the RPARPAR peptide immobilized on agarose beads. Elution with a buffer containing free RPARPAR peptide released a 130-kDa protein (Fig. 4*A*, *Top*), which was identified by MALDI-TOF mass spectroscopy and confirmed by immunoblotting as NRP-1 (Fig. 4*A*, *Bottom*). M21 melanoma cells (27), which we found not to express NRP-1, did not bind or internalize RPARPAR phage. Forced expression of NRP-1 rendered these cells capable of binding RPARPAR phage (Fig. 4*B*). Confocal microscopy showed that RPARPAR phage colocalized with NRP-1 at the cell surface and inside the NRP-1–transfected M21 cells (Fig. 4*C*, green cells) but not nontransfected M21 cells (Fig. 4*C*, dark cells indicated by asterisks). M21 cells transfected with NRP-1 containing inactivating mutations in the b1 domain, which is involved in VEGF binding (28), did not bind RPARPAR phage (Fig. 4*B*). A recent publication described cyclic peptides that bind to NRP-1 but contain an internal, not C-terminal, CendR motif (29). Because these results do not seem to agree with the C-end rule, we generated phage clones displaying one of these peptides, CRRPRMLTC, and its fragment with

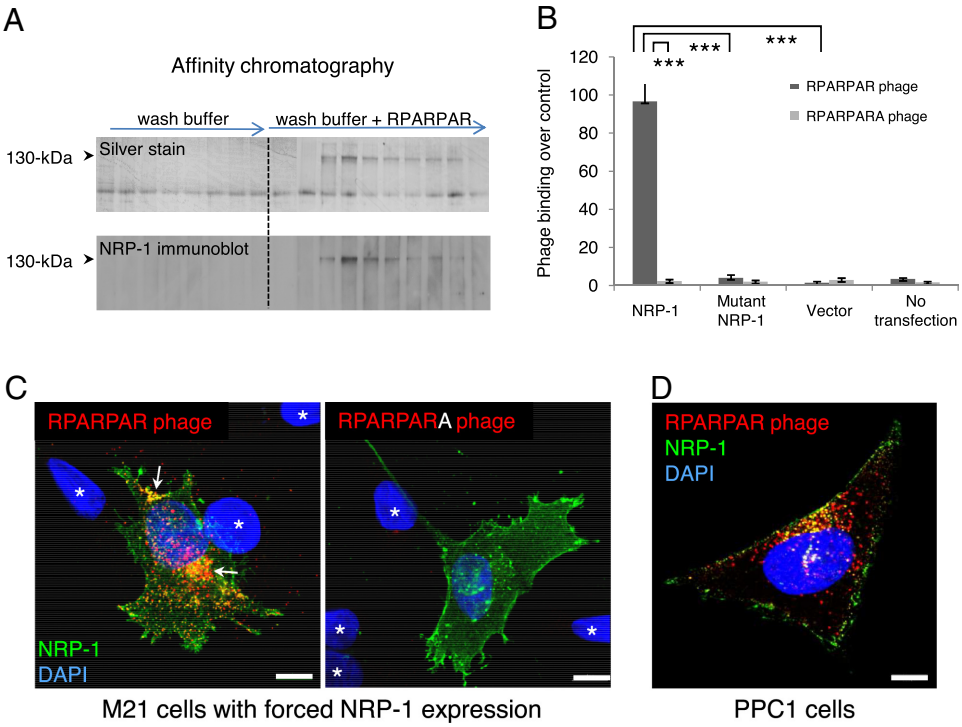

Fig. 4. Identification and validation of NRP-1 as the CendR receptor. (*A*) Affinity chromatography of proteins interacting with RPARPAR peptide. PPC-1 tumor tissue was extracted with a 200 mM glucopyranoside buffer, and the extract was incubated with RPARPAR peptide-coated beads, followed by extensive washing and elution with 2 mM free RPARPAR peptide. *Top*: A silver-stained gel. Note the appearance of a 130-kDa band, after elution with the free RPARPAR peptide. *Bottom*: An immunoblot with an anti-NRP-1 antibody. (*B*) Binding of RPARPAR phage to M21 melanoma cells transiently transfected with wild-type NRP-1 (NRP-1), triple mutant NS346A-E348A-T349A NRP-1 (Mutant NRP-1), or parental pcDNA3.1 plasmid (Vector), and to nontransfected M21 cells. Statistical analysis was performed with ANOVA; $n = 3$; error bars indicate SEM; ***, $P < 0.001$. (*C*) Internalization of RPARPAR phage into M21 cells transiently transfected with NRP-1. RPARPAR phage (*Left*) or RPARPARA phage (*Right*) was incubated with the cells for 3 h at 37 °C. RPARPAR phage is internalized into NRP-1–expressing cells (*Left*, arrows) but not into the NRP-1–negative cells (*Left*, asterisks). RPARPARA phage is not internalized into NRP-1–positive M21 cells (*Right*). (*D*) A confocal immunofluorescence image of NRP-1 and RPARPAR phage in PPC-1 cells incubated with phage at 37 °C for 3 h. (*C* and *D*) Green, NRP-1; red, phage; blue, DAPI. (Scale bars, 10 μm.)

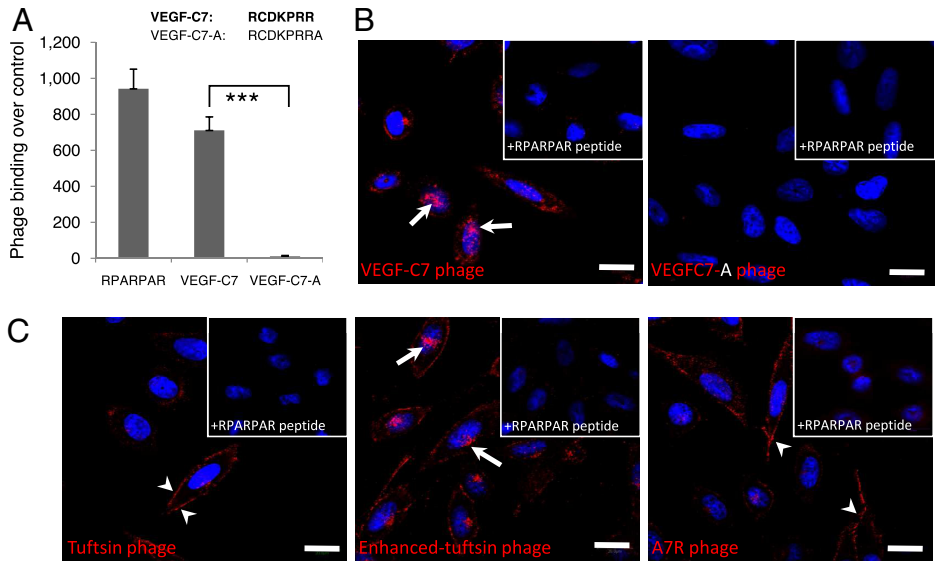

Fig. 5. Binding of phage displaying NRP-1 ligand peptides to PPC-1 cells. (*A*) Phage displaying the C-terminal 7 aa of VEGF (VEGF-C7) binds to PPC1 cells; adding a C-terminal alanine to the peptide (VEGF-C7-A) eliminates the binding. Statistical analysis was performed by Student's *t* test. $n = 3$; error bars indicate SEM; ***, $P < 0.001$. (*B* and *C*) Phage immunoreactivity in PPC1 cells. The cells were cultured for 1 h in the presence of 10^9 pfu of phage expressing the indicated peptides, stained with anti-T7 antibodies (red), and examined by confocal microscopy. Nuclei were stained with DAPI (blue). *Insets*: Competition of the phage binding by 0.5 mM free RPARPAR peptide (added to the cells 10 min before adding the phage). (Scale bars, 20 μm.)

exposed CendR element (CRRPR), and tested their binding to PPC-1 cells. The CRRPRMLTC phage bound slightly, but reproducibly, to the cells, whereas the CRRPR phage showed robust binding that was almost completely inhibited by oligomeric RPARPAR peptide (Fig. S7). The binding of the CRRPRMLTC phage was not significantly inhibited by RPARPAR. These data indicate that the CRRPRMLTC peptide interacts weakly, if at all, with the CendR-binding pocket of NRP-1, which is optimal for binding of peptides with C-terminal arginine residues (28).

Affinity measurement indicated a $K_d = 1.7 \pm 0.4$ μM for the binding of the RPARPAR peptide to purified NRP-1 (Fig. S8). The interaction was specific, because it was inhibited by an excess of unlabeled RPARPAR peptide but not by an excess of RARPARA, RPARPAR-NH_2, or D-rparpar peptides (Fig. S8*B*). These results are in agreement with the cell-binding experiments shown in Fig. S3, which demonstrate that RPARPAR binding requires the presence of C-terminal arginine with a free carboxyl group and that only L-amino acid peptides are active.

CendR Peptides Share an Active Site with the C Terminus of VEGF-A165. A known ligand of NRP-1, VEGF-A165, interacts with NRP-1 through a C-terminal CendR-like sequence (CRCDKPRR) (22, 30). T7 phage displaying the 7 C-terminal amino acids of VEGF-A165 bound to (Fig. 5*A*) and was internalized into PPC1 cells (Fig. 5*B*, *Left*). The internalization was reduced in the presence of unlabeled RPARPAR peptide (Fig. 5*B*, *Left inset*). As was the case with RPARPAR, the ability of the CRCDKPRR phage to promote cell binding (Fig. 5*A*) and internalization (Fig. 5*B*, *Right*) was lost when an alanine residue was added to the C terminus. These results show that the C terminus of VEGF contains an active CendR element. Several peptides with C-terminal arginine, such as tuftsin (TKPR), enhanced tuftsin (TKPPR), and A7R (ATWLPPR), are known to compete with VEGF for NRP-1 interaction (31, 32). T7 phage clones displaying these peptides also bound to PPC1 cells, and the binding was inhibited by the free RPARPAR peptide (Fig. 5*C*) and RPARPAR rendered tetrameric using neutravidin (Fig. S9), indicating a shared binding site.

CendR Peptides Cause Vascular Leakage and Tissue Penetration. NRP-1 is a known mediator of vascular permeability induced by VEGF and certain semaphorins (20, 21, 33). Our observation that RPARPAR phage extravasates and spreads into the lung parenchyma in vivo led us to test the possibility that the CendR peptide–NRP-1 interaction could regulate vascular permeability. We used a modified Miles vascular leakage assay to evaluate the extravasation of tracers of different sizes (an albumin-binding dye, Evans blue; firefly luciferase, 62 kDa; and T7 phage, 50,000 kDa) from dermal microvessels. The RPARPAR peptide increased vascular leakage of the tracers at the injection site at millimolar concentrations (Fig. S10). Multimeric RPARPAR peptides, rendered polyvalent using neutravidin or qdots as a scaffold, were much more effective, triggering vascular leakage at >100-fold lower concentrations of the peptide. In addition to increasing the avidity of the interaction, multimeric RPARPAR may also have qualitatively different effects, for example through receptor clustering. The high concentrations of RPARPAR peptide needed for the vascular leakage effect may be related to rapid dilution and clearance of the peptide at the injection site. Preinjecting a blocking anti–NRP-1 antibody suppressed the permeabilizing effect (Fig. 6 *A*–*C*), indicating that RPARPAR acts through NRP-1. Histologic analysis confirmed the extravasation of phage from the dermal microvessels at the injection site (Fig. 6*D*).

Finally, to study the ability of systemically delivered oligomeric CendR peptides to cause vascular leakage, we injected neutravidin–RPARPAR complexes i.v. into mice and determined the tissue distribution of coinjected tracer phage. Neutravidin–RPARPAR, but not a similar control peptide construct, caused increased retention of the phage in lungs and other organs (Fig. S11). These results are in line with the in vivo tissue distribution of systemically injected RPARPAR-phage, showing that it accumulates in the first-met vascular beds.

Discussion

Our study reveals a cell, vascular, and tissue penetration pathway that we have termed CendR. The salient features of CendR are (*i*) R/KXXR/K recognition motif, (*ii*) requirement for C-terminal exposure of the motif for activity, (*iii*) conversion of internal CendR motifs into active, C-terminal ones through proteolytic cleavage, and (*iv*) NRP-1 dependence of the recognition and penetration activities.

Our phage library screens on tumor-derived cells gave the surprising result that the diversity of the libraries almost completely collapsed into CendR motif sequences. The likely reason why this phenomenon has not been noted before is the strict requirement for the CendR motif to be at the C terminus of the peptide for cell binding to occur. Such peptides can be obtained in the T7 phage random display system because the peptides are expressed at the C terminus of the phage coat protein (24). In contrast, in the more commonly used filamentous phage, peptides are displayed at the N

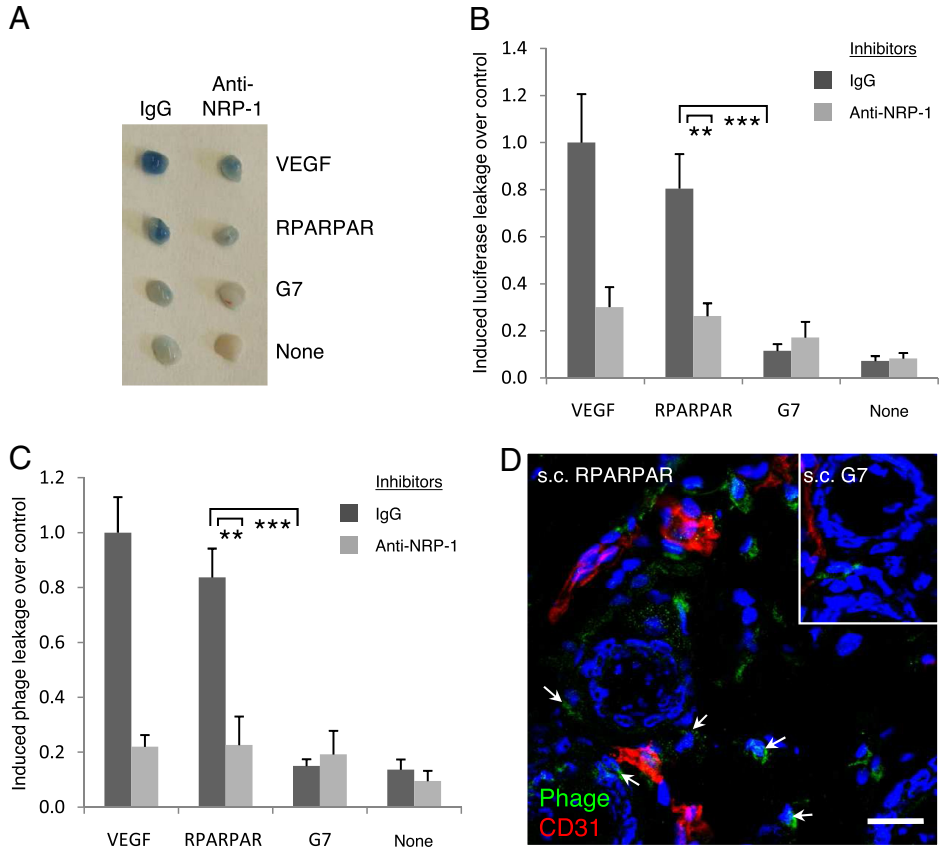

Fig. 6. Multimeric CendR peptides cause leakage in blood vessels and tissue penetration. (*A*) Miles assay: Macroscopic appearance of Evans blue leakage in skin samples of mice preinjected intradermally with PBS containing either goat IgG (left column) or anti–NRP-1 neutralizing antibodies (right column), followed 20 min later by injection of PBS containing 50 ng VEGF-165, multimeric RPARPAR (qdot scaffold; peptide concentration, 8 μM), multimeric G7 peptide (qdot scaffold; peptide concentration, 1.2 μM), or only PBS (None). (*B*) Quantification of vascular leakage of luciferase in dermal samples. Luciferase activity in VEGF-injected skin was set to equal 1 as a control. (*C*) Quantification of vascular leakage of tracer phage in dermal samples. Phage titer in VEGF-injected skin was set to equal 1 as a control. Statistical analysis was performed by Student's *t* test; $n = 4$; error bars indicate SEM; **, $P < 0.01$; ***, $P < 0.001$. (*D*) Confocal microscopy of phage immunoreactivity (green) and blood vessels (CD31 staining; red) reveals phage leakage into the dermis of mice injected with multimeric RPARPAR, but not G7 (*Inset*).

terminus of one of the phage proteins (34), which means that this system cannot yield peptides with an exposed C terminus. We show in several ways that NRP-1 is the molecule responsible for the binding of CendR peptides and initiates the subsequent internalization and permeability effects. Binding experiments at the purified protein and cellular levels, and antibody inhibition, confirmed the initial identification of NRP-1 as a CendR receptor by affinity chromatography. The known binding specificity of NRP-1 also agrees with a role as a CendR receptor. The peptide motif at the C terminus of VEGF-A165 that mediates the binding of this VEGF form to NRP-1 contains a C-terminal arginine and a CendR motif, and that is also the case with several other natural and artificial ligands of NRP-1. The structure of the binding pocket in the b1 domain of NRP-1 has been determined and seems to optimally accommodate a C-terminal arginine (28). The role of the internal basic amino acid in the R/KXXR/K motif may be related to stabilization of the peptide–NRP-1 complex. The observation that enhanced tuftsin (T**KPPR**) binds to endothelial cells approximately 20-fold more avidly than tuftsin (TKP**R**) (31) agrees with the importance of spacing of the basic residues in the NRP-1 interaction suggested by our phage-derived sequences.

Our antibody inhibition experiments suggested that NRP-1 is the sole or at least the main CendR receptor in tissues, because an anti-NRP-1 antibody inhibited the vascular permeability effect of CendR peptides by 70–80%. Neuropilin-2 also binds VEGF-A165 through the C-terminal CendR domain. However, the binding specificities of the 2 neuropilins with VEGFs other than VEGF-A165 and semaphorins, although overlapping, do not seem to be identical (19). Thus, it may be possible to develop CendR peptides that are recognized by one neuropilin but not the other.

The peptides that have been previously shown to bind to the b1 domain site in NRP-1 have been viewed as competitors of endogenous NRP-1 ligands. Our results show that CendR peptides have cell-penetrating properties and can cause vascular leakage and tissue penetration in vivo. Many cationic CPPs (5) contain active or cryptic CendR elements, and the TAT peptide binds to the same binding site in NRP-1 as VEGF (34). Moreover, our data show that cell binding of TAT peptide-displaying phage to PPC1 cells can be blocked with RPARPAR peptide and RPARPAR-coated qdots. However, there are major differences between CendR peptides and cationic CPPs: CPPs composed of D-amino acids are active (25, 26), whereas our results show that CendR uptake is dependent on specific recognition of L-peptides only. In addition, many of the CPPs can internalize cargo anchored C-terminal of the CendR element in a manner that is not compatible with CendR-induced internalization. We suggest that the CendR pathway, although capable of internalizing at least some of the cationic CPPs, is not the major mechanism for the cell-penetrating activity of CPPs.

We show that the interaction of the CendR peptide RPARPAR with NRP-1 can cause vascular leakage in vivo. The involvement of NRP-1 in the regulation of vascular permeability is well established (20, 21, 33). The RPARPAR peptide was particularly effective in this regard when assembled into a multimeric construct. The likely reason is that the K_d of CendR peptides is in a low-micromolar range, and the avidity of a multivalent complex compensates for the low affinity of the individual peptides. It may also be that effective NRP-1 signaling requires receptor dimerization or multimerization, which the multivalent CendR constructs would likely induce more effectively than the monovalent peptides. The cell-internalizing and vascular-penetrating activities of CendR peptides are possibly mechanistically related. One of the pathways of VEGF-mediated vascular leakage involves a transcellular route through a maze of conduits termed *vesiculo-vacuolar organelles* (35). It may be that the CendR peptides also activate this pathway. Remarkably, our results show that a cargo coupled to a CendR peptide not only escapes from the vasculature but also spreads beyond the immediate vicinity

of blood vessels. It seems that CendR peptide can traverse through both vascular and parenchymal cells to penetrate into tissues.

Proteolytic cleavage of viral coat proteins with concomitant exposure of CendR elements seems to be a recurring theme in tissue spreading and infectivity of many viruses (Table S1). Pathologic vascular edema is associated with many disease states, such as hemorrhagic virus infections, sepsis, and organ-specific vascular leakage syndromes (36, 37). Compounds that block the CendR interaction may provide tools for intervention in such diseases. Finally, it may be possible to achieve CendR-mediated internalization and tissue penetration by combining docking-based targeting modules with protease-sensitive CendR targeting elements.

Materials and Methods

Animal Procedures. All of the animal experimentation was performed with BALB/c nude mice (Harlan Sprague–Dawley) according to procedures approved by the Animal Research Committee at University of California, Santa Barbara.

Phage Display. For in vivo phage display, mice were injected i.v. with 10^{10} pfu of T7 phage followed by perfusion of the circulatory system and determination of the bound phage in target organs by titration. For cell-binding studies on cultured cells (in vitro display) and organ-derived cell suspensions (*ex vivo* display), the cells were incubated with 10^9 pfu of phage at 4 °C, washed, lysed, and quantified by titration. Incubation at 37 °C followed by low-pH wash (glycine-HCl, pH 2.5) was used to assess the amount of internalized phage.

Labeling of Qdots. Biotinylated peptides were used to functionalize the 605 ITK streptavidin qdots (Invitrogen) according to the manufacturer's instructions.

Immunofluorescence. Cultured cells and tissue sections were fixed with 4% buffered paraformaldehyde or cold (−20 °C) methanol followed by incubations with appropriate primary and Alexa-labeled secondary antibodies and nuclear staining with DAPI or Hoechst 342 DNA dyes.

Affinity Chromatography. PPC1 tumors were lysed in PBS containing 200 mM n-octyl-beta-D-glucopyranoside, and clarified lysates were incubated with RPARPAR-coated Sulfolink-beads (Pierce). After washing, bound proteins were eluted with lysis buffer containing 2 mM free RPARPAR peptide and separated by SDS-PAGE. Gel fragments excised from silver-stained gel of eluted fractions were subjected to MALDI-TOF mass spectrometry at the Burnham Institute for Medical Research Proteomics Resource.

Statistical Analysis. Data were analyzed by Student's *t* test and 1-way ANOVA, followed by a suitable post hoc test.

ACKNOWLEDGMENTS. We thank Drs. Eva Engvall, Elena Pasquale, and Douglas Hanahan for their critical reading of the manuscript; Dr. Michael Klagsbrun for the NRP-1 cDNA construct; Dr. David Cheresh for the M21 cell line; Roslind Varghese for editing; and Dr. Lianglin Zhang, Dr. Tero Järvinen, Christopher B. Brunquell, and Olivia M. Yu for their help with the phage display experiments. This work was supported by National Cancer Institute Grants CA104898, CA115410, CA119414, and CA119335 and U.S. Department of Defense Grant W81XWH-08–1-0727.

1. Joliot A, Pernelle C, Deagostini-Bazin H, Prochiantz A (1991) Antennapedia homeobox peptide regulates neural morphogenesis. *Proc Natl Acad Sci USA* 88:1864–1868.
2. Elliott G, O'Hare P (1997) Intercellular trafficking and protein delivery by a herpesvirus structural protein. *Cell* 88:223–233.
3. Green M, Loewenstein PM (1988) Autonomous functional domains of chemically synthesized human immunodeficiency virus tat trans-activator protein. *Cell* 55:1179–1188.
4. Frankel AD, Pabo CO (1988) Cellular uptake of the tat protein from human immunodeficiency virus. *Cell* 55:1189–1193.
5. Langel Ü (2007) *Handbook of Cell-Penetrating Peptides* (CRC/Taylor & Francis, Boca Raton).
6. Laakkonen P, Porkka K, Hoffman JA, Ruoslahti E (2002) A tumor-homing peptide with a targeting specificity related to lymphatic vessels. *Nat Med* 8:751–755.
7. Porkka K, Laakkonen P, Hoffman JA, Bernasconi M, Ruoslahti E (2002) A fragment of the HMGN2 protein homes to the nuclei of tumor cells and tumor endothelial cells in vivo. *Proc Natl Acad Sci USA* 99:7444–7449.
8. Hoffman JA, et al. (2003) Progressive vascular changes in a transgenic mouse model of squamous cell carcinoma. *Cancer Cell* 4:383–391.
9. Järvinen TA, Ruoslahti E (2007) Molecular changes in the vasculature of injured tissues. *Am J Pathol* 171:702–711.
10. Jiang T, et al. (2004) Tumor imaging by means of proteolytic activation of cell-penetrating peptides. *Proc Natl Acad Sci USA* 101:17867–17872.
11. Michel CC (1996) Transport of macromolecules through microvascular walls. *Cardiovasc Res* 32:644–653.
12. Rabbani ML, Rogers PA (2001) Role of vascular endothelial growth factor in endometrial vascular events before implantation in rats. *Reproduction* 122:85–90.
13. Maeda H, Fang J, Inutsuka T, Kitamoto Y (2003) Vascular permeability enhancement in solid tumor: Various factors, mechanisms involved and its implications. *Int Immunopharmacol* 3:319–328.
14. Baban DF, Seymour LW (1998) Control of tumour vascular permeability. *Adv Drug Deliv Rev* 34:109–119.
15. Senger DR, et al. (1983) Tumor cells secrete a vascular permeability factor that promotes accumulation of ascites fluid. *Science* 219:983–985.
16. Ferrara N, Henzel WJ (1989) Pituitary follicular cells secrete a novel heparin-binding growth factor specific for vascular endothelial cells. *Biochem Biophys Res Commun* 161:851–858.
17. Ferrara N, Gerber HP, LeCouter J (2003) The biology of VEGF and its receptors. *Nat Med* 9:669–676.
18. Takashima S, et al. (2002) Targeting of both mouse neuropilin-1 and neuropilin-2 genes severely impairs developmental yolk sac and embryonic angiogenesis. *Proc Natl Acad Sci USA* 99:3657–3662.
19. Staton CA, Kumar I, Reed MWR, Brown NJ (2007) Neuropilins in physiological and pathological angiogenesis. *J Pathol* 212:237–248.
20. Becker PM, et al. (2005) Neuropilin-1 regulates vascular endothelial growth factor-mediated endothelial permeability. *Circ Res* 96:1257–1265.
21. Acevedo LM, Barillas S, Weis SM, Göthert JR, Cheresh DA (2008) Semaphorin 3A suppresses VEGF-mediated angiogenesis yet acts as a vascular permeability factor. *Blood* 111:2674–2680.
22. Jia H, et al. (2006) Characterization of a bicyclic peptide neuropilin-1 (NP-1) antagonist (EG3287) reveals importance of vascular endothelial growth factor exon 8 for NP-1 binding and role of NP-1 in KDR signaling. *J Biol Chem* 281:13493–13502.
23. Starzec A, et al. (2006) Antiangiogenic and antitumor activities of peptide inhibiting the vascular endothelial growth factor binding to neuropilin-1. *Life Sci* 79:2370–2381.
24. Hoffman JA, Laakkonen P, Porkka K, Bernasconi M, Ruoslahti E (2004) In vivo and ex vivo selections using phage-displayed libraries. *Phage Display: A Practical Approach*, eds Clackson T, Lowman HB (Oxford Univ Press, Oxford), Chap 10.
25. Wadia JS, Dowdy SF (2002) Protein transduction technology. *Curr Opin Biotech* 13:52–56.
26. Gammon ST, Villalobos VM, Prior JL, Sharma V, Piwnica-Worms D (2003) Quantitative analysis of permeation peptide complexes labeled with Technetium-99m: Chiral and sequence-specific effects on net cell uptake. *Bioconjug Chem* 14:368–376.
27. Cheresh DA, Spiro RC (1987) Biosynthetic and functional properties of an Arg-Gly-Asp-directed receptor involved in human melanoma cell attachment to vitronectin, fibrinogen, and von Willebrand factor. *J Biol Chem* 262:17703–17711.
28. Vander Kooi CW, et al. (2007) Structural basis for ligand and heparin binding to neuropilin B domains. *Proc Natl Acad Sci USA* 104:6152–6157.
29. Hong TM, et al. (2007) Targeting neuropilin 1 as an antitumor strategy in lung cancer. Clin Cancer Res 13:4759–4768.
30. Soker S, Takashima S, Miao HQ, Neufeld G, Klagsbrun M (1998) Neuropilin-1 is expressed by endothelial and tumor cells as an isoform-specific receptor for vascular endothelial growth factor. *Cell* 92:735–745.
31. von Wronski MA, et al. (2006) Tuftsin binds neuropilin-1 through a sequence similar to that encoded by exon 8 of vascular endothelial growth factor. *J Biol Chem* 281:5702–5710.
32. Starzec A, et al. (2007) Structure-function analysis of the antiangiogenic ATWLPPR peptide inhibiting VEGF(165) binding to neuropilin-1 and molecular dynamics simulations of the ATWLPPR/neuropilin-1 complex. *Peptides* 28:2397–2402.
33. Mamluk R, Klagsbrun M, Detmar M, Bielenberg DR (2005) Soluble neuropilin targeted to the skin inhibits vascular permeability. *Angiogenesis* 8:217–227.
34. Jia H, et al. (2001) Cysteine-rich and basic domain HIV-1 Tat peptides inhibit angiogenesis and induce endothelial cell apoptosis. *Biochem Biophys Res Commun* 283:469–479.
35. Dvorak AM, Feng D (2001) The vesiculo-vacuolar organelle (VVO). A new endothelial cell permeability organelle. *J Histochem Cytochem* 49:419–432.
36. Basu A, Chaturvedi UC (2008) Vascular endothelium: The battlefield of dengue viruses. *FEMS Immunol Med Microbiol* 53:287–299.
37. Weis SM (2008) Vascular permeability in cardiovascular disease and cancer. *Curr Opin Hematol* 15:243–249.